

Figure S1. Ebastine decreases EZH2 and H3K27 methylation levels in cancer.

(A) MCF7 cells were treated with Astemizole, Chlorpheniramine, Ebastine, Fexofenadine, Haloperidol at various doses as indicated in addition to DMSO for 72 h and lysed for immunoblot analysis. (B) H82, H526, VCaP, Jeko-1, and HDLM2 cells treated with ebastine for 72 h were lysed for immunoblot analysis.

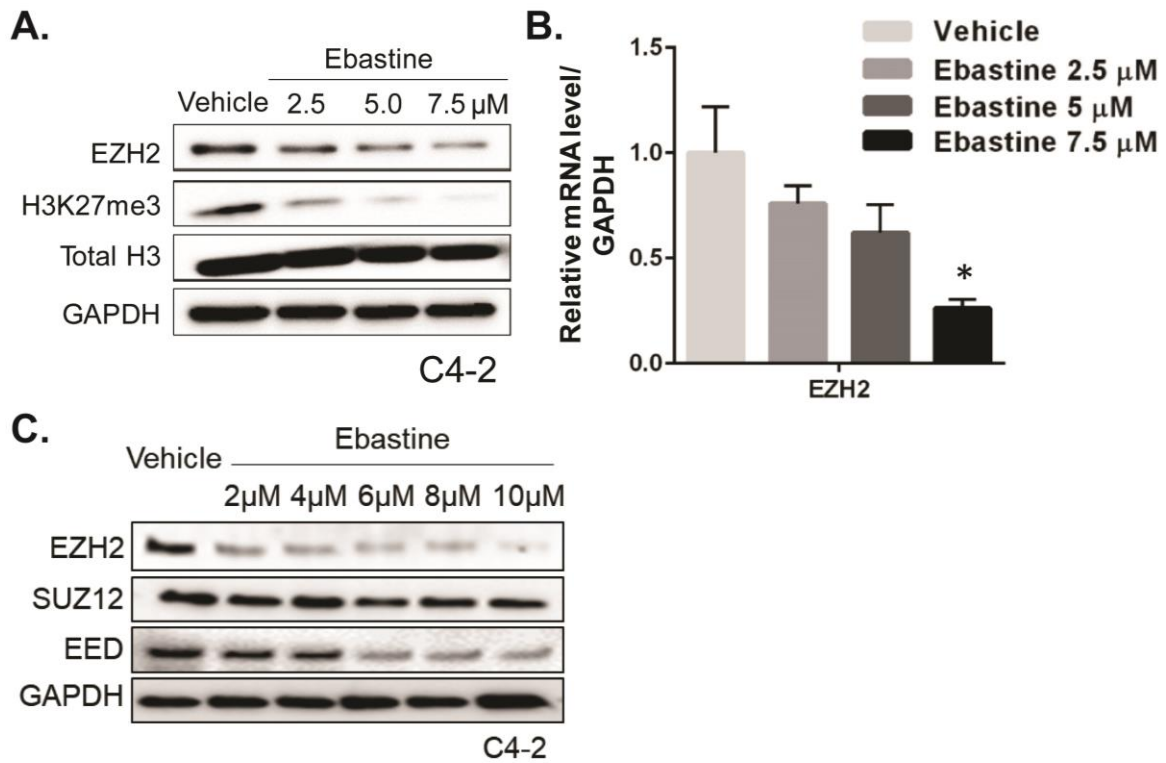


Figure S2. Ebastine decreased EZH2 protein and transcript levels in C4-2 cells.

C4-2 cells treated with ebastine at dose gradients for 72 h were lysed for immunoblot analysis (A) and RT-qPCR (B) (* $P < 0.05$, mean \pm SEM). C4-2 cells were treated with ebastine at dose gradients. After 72 h, total cell lysates were blotted for EZH2, SUZ12 and EED, while GAPDH served as the loading control (C).

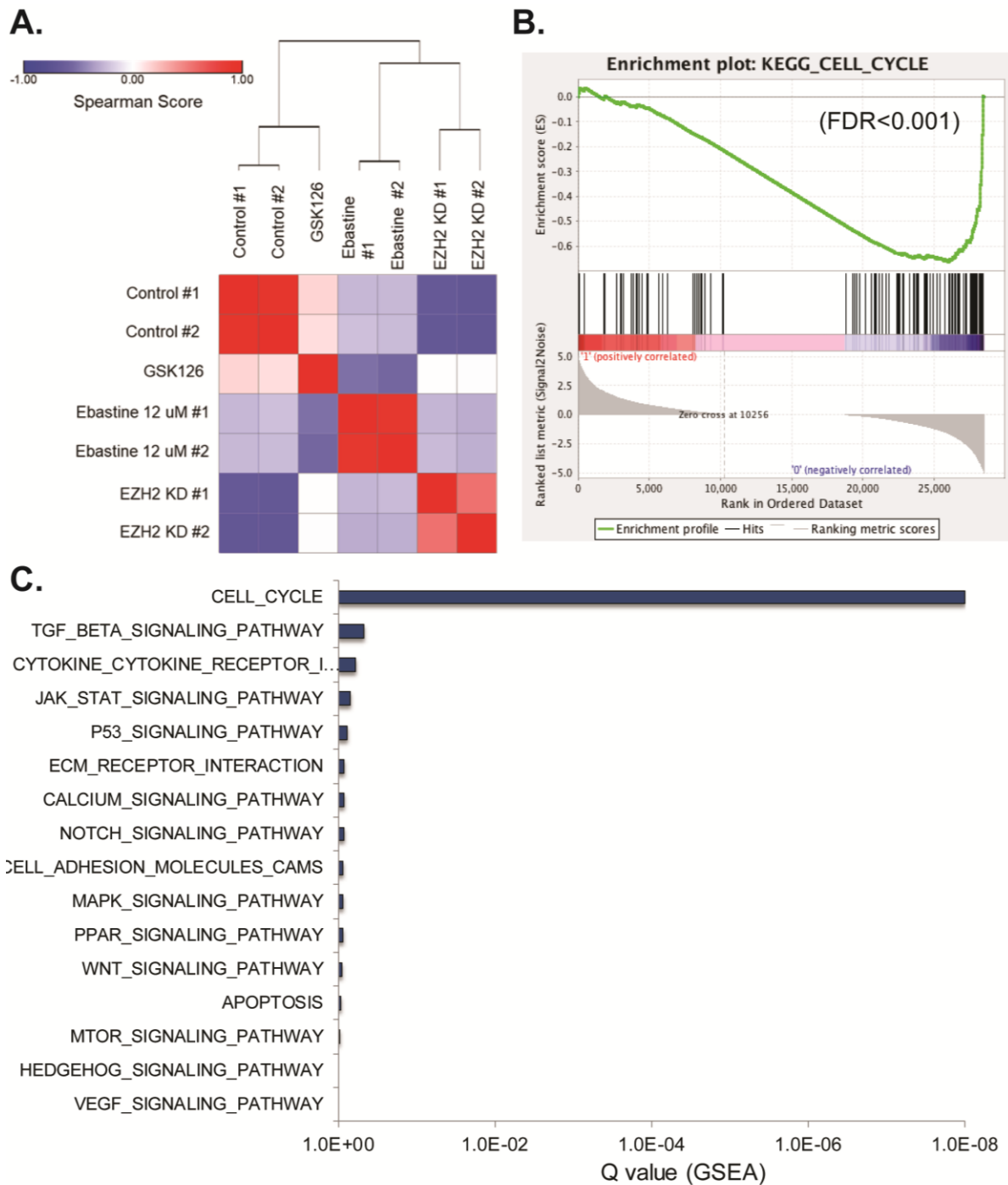


Figure S3. Additional RNaseq data on GSK126, ebastine, and EZH2-KD. (A) Ebastine 12 μ M treatment and EZH2 KD samples cluster together. (B) Cell cycle pathway is down-regulated after Ebastine treatment (FDR<0.001). (C) Cell cycle is the most significantly enriched cancer-related pathway after Ebastine treatment.

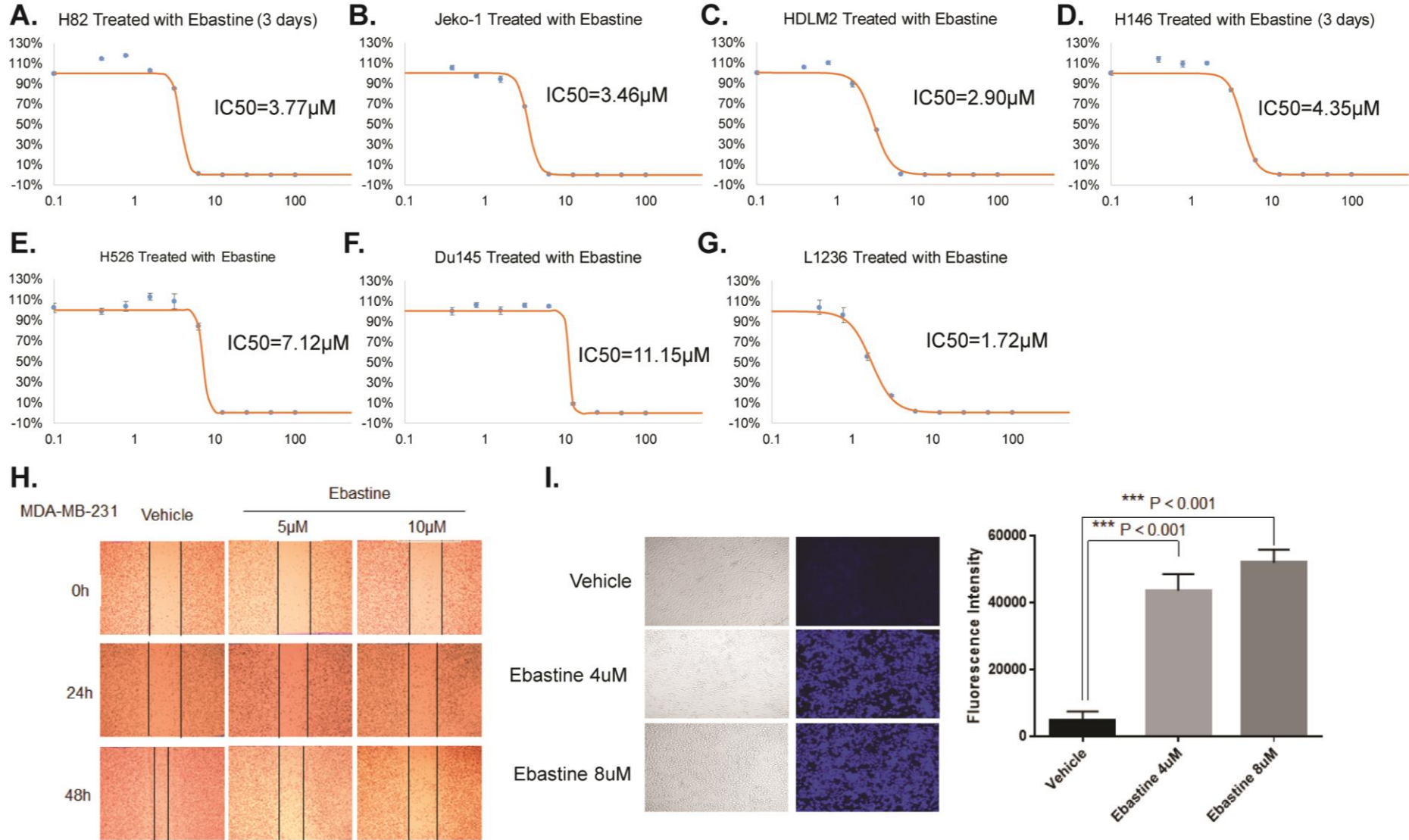


Figure S4. Ebastine inhibits proliferation, migration, and induces autophagy in cancer cells.

(A-G) Growth curves of H82, Jeko-1, HDLM2, H146, H526, DU145 and L1236 after treated with ebastine for 72 h. (H) Wound healing assay for migrating ability of MDA-MB-231 cells after ebastine treatment. (I) Autophagosome staining in C4-2 cells after ebastine treatment. Upper panel: Specific blue fluorescence staining of autophagosome due to ebastine treatment. Lower panel: Quantification of fluorescence intensity to indicate autophagy induced by ebastine in a dose-dependent manner (unpaired t-test, n=10, mean \pm SEM).

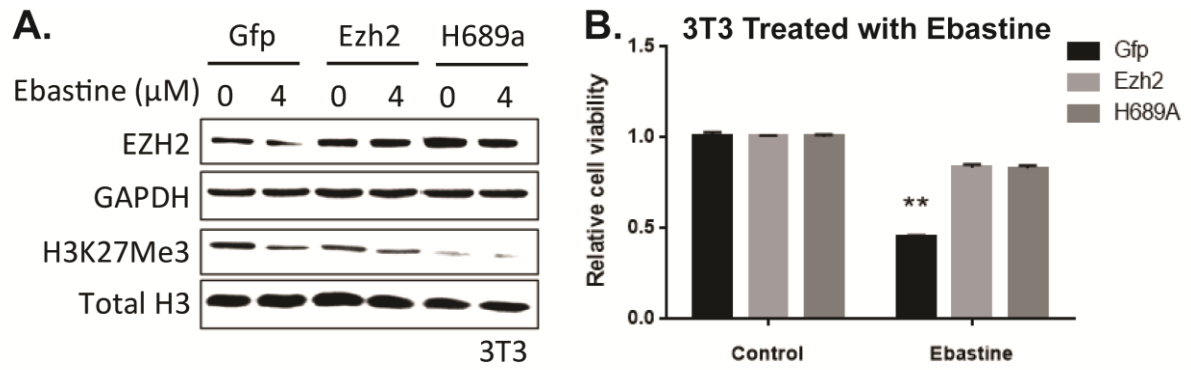


Figure S5. Overexpression of EZH2 and its mutant H689A mitigates the effect of ebastine .

Ezh2 wild-type and H689A mutant overexpressed NIH3T3 cells were provided by Dr. Yi Zhang. Cells were treated with 4 μM ebastine for 72 h to measure the protein levels (A) and proliferative potential of the cells (B). Total cell lysate was blotted for EZH2 and H3K27me3, with H3 and GAPDH as the loading control. Data are presented as mean \pm SEM and * represent $P < 0.05$.

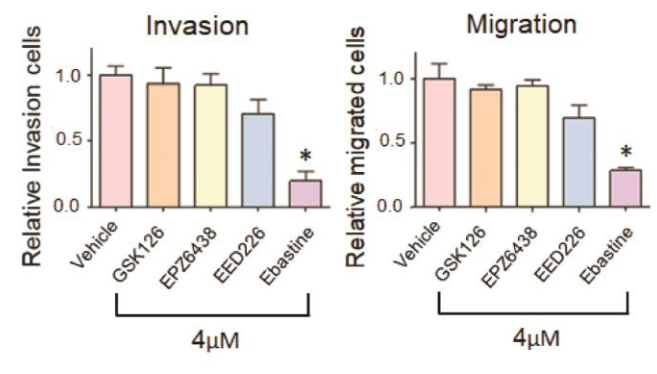
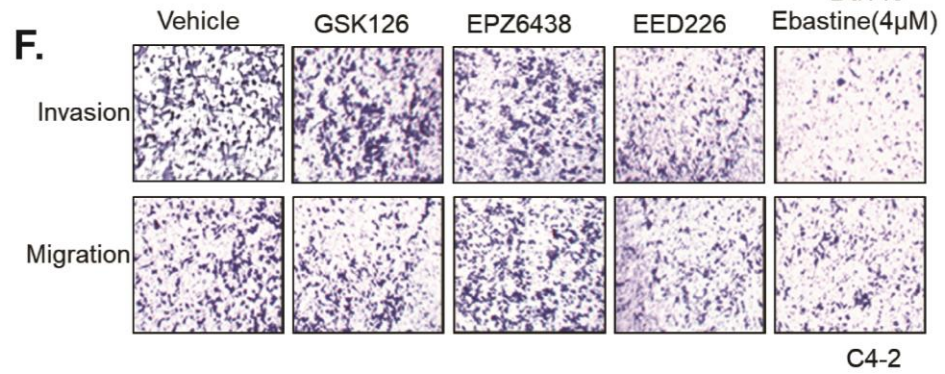
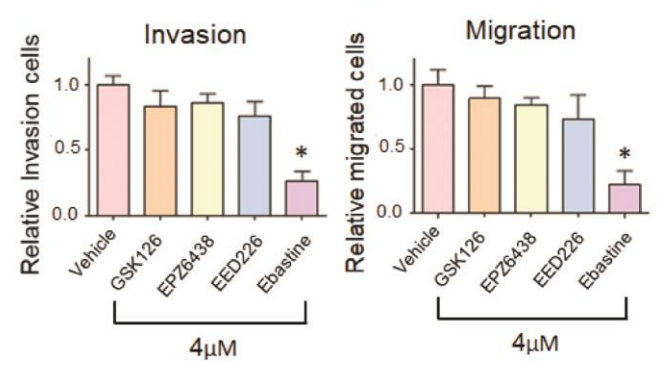
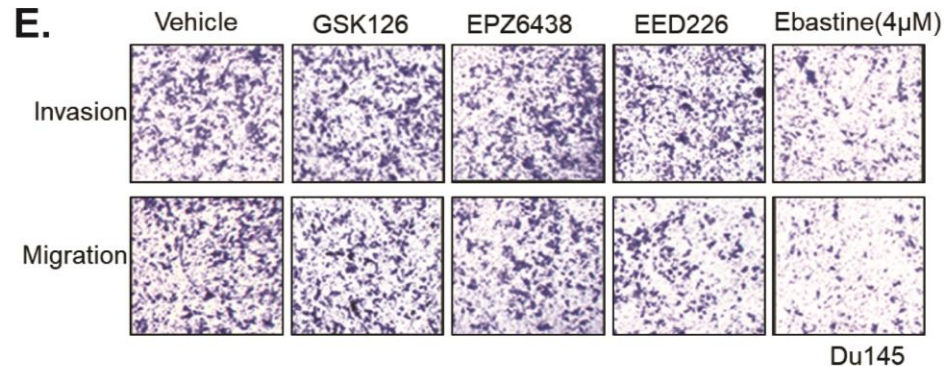
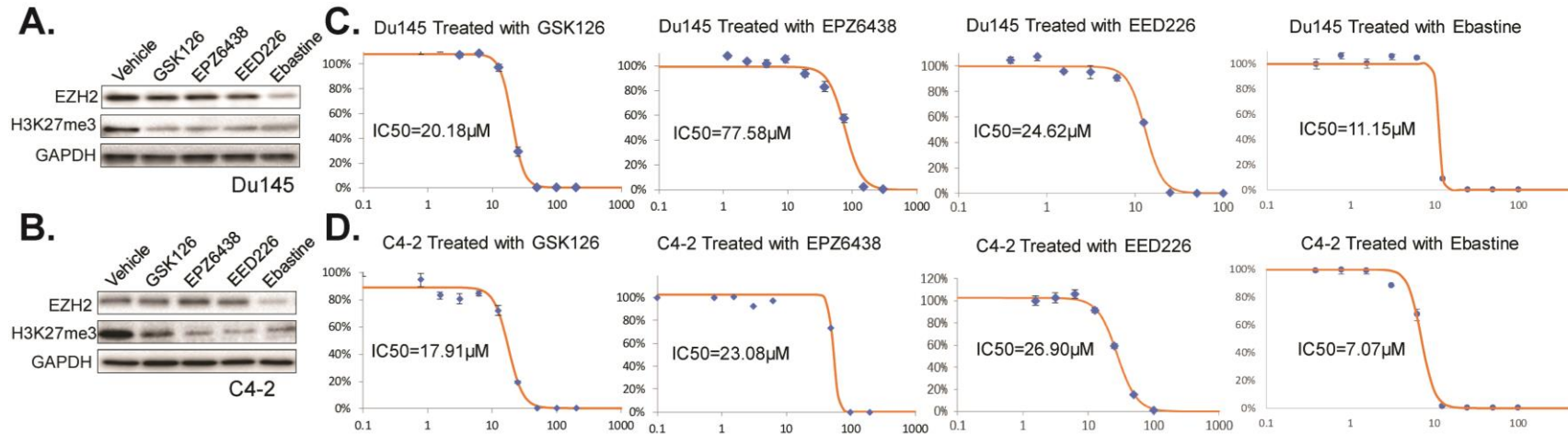
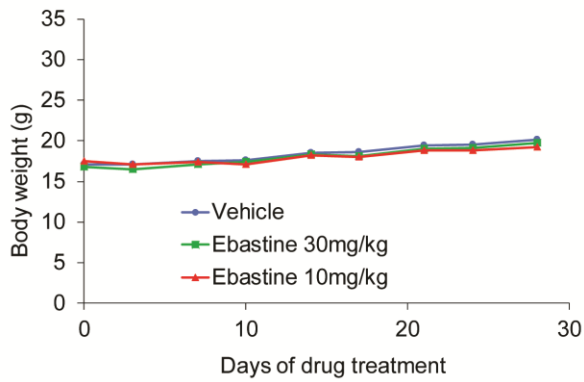


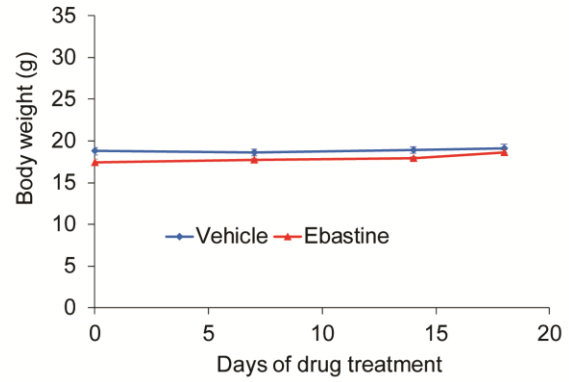
Figure S6. Ebastine has strong anti-cancer activities than other EZH2 enzyme inhibitors.

(A, B) The protein level of EZH2 and H3K27 in Du145 (A) and C4-2 (B) prostate cancer cells after treated with 4 μ M of GSK126, EPZ6438, EED226, and ebastine for 72 h. (C, D) The growth curves of Du145 (C) and C4-2 (D) cells after Ebastine and EZH2 enzyme inhibitor treatment at 4 μ M for 72 h. (E, F) Invasion and migration assay of Du145 (E) and C4-2 (F) cells after ebastine and EZH2 enzyme inhibitor treatments at 4 μ M for 72 h. Data are presented as mean \pm SEM and * represent $P < 0.05$.

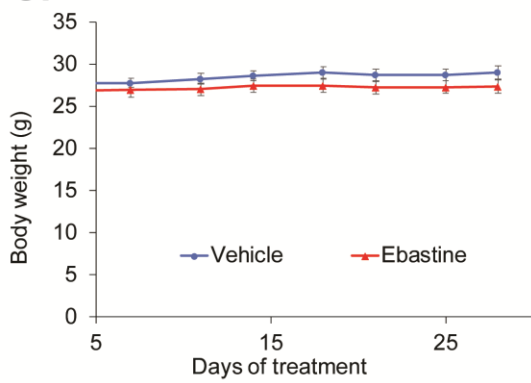
A. 3887LM TG6 xenograft model



B. SUM159 xenograft model



C. VCaP xenograft model



D. LuCaP 35CR xenograft model

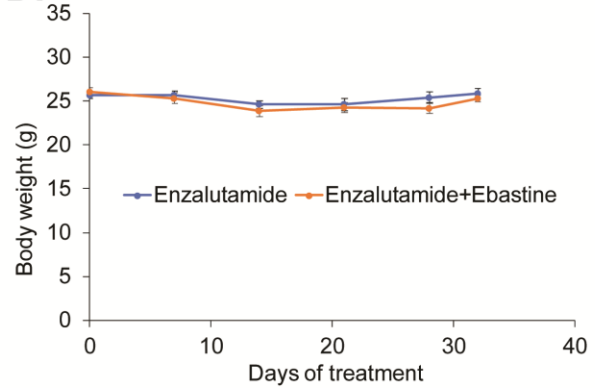


Figure S7. Ebastine treatment did not alter the body weight of mice.

Oral administration of ebastine did not change the body weight of mice in the 3887LM TG6 (A), SUM159 (B), VCaP (C), and LuCaP 35CR (D) xenograft model.

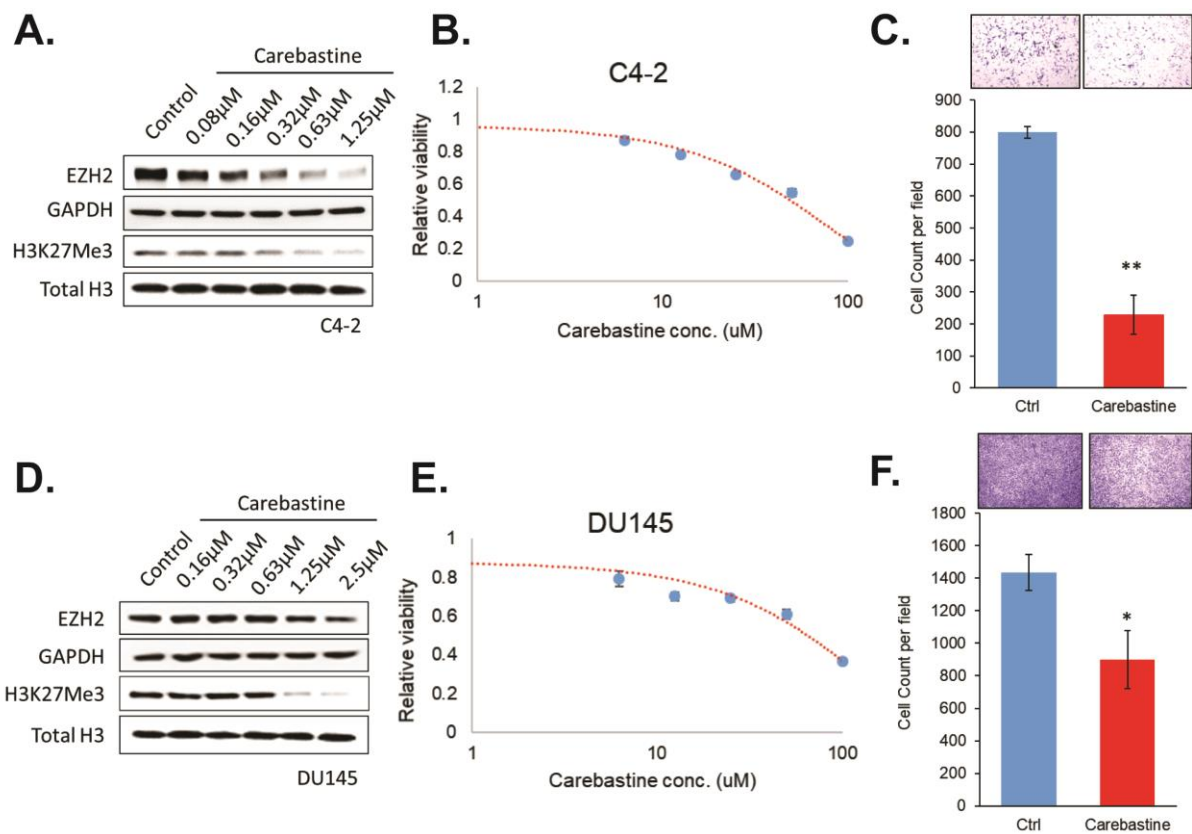


Figure S8. Carebastine, a metabolite of ebastine, reduces EZH2 protein level and inhibits cancer cell growth and invasion in prostate cancer cells.

(A-C) C4-2 cells treated with carebastine at different doses for 72 h and measured protein level (A), cell growth (B), and invasion (C). (D-F) Du145 cells treated with carebastine at different doses for 72 h and measured protein level (D), cell growth (E), and invasion (F). Data are presented as mean \pm SEM and * represent $P < 0.05$.